# Development of a Novel Melanoma Detection Model Using Deep Learning

Sheenam[1], Bobbinpreet Kaur[2], Bhawna Goyal[2,3], Ayush Dogra[4], Vinay Kukreja[4,*], Mustafa Asaad Rasol[5], and Aqeel Ali[6]

ARTICLE INFO

*Article history:*
Received: 14 October 2023
Revised: 15 March 2024
Accepted: 28 May 2024
Online: 30 June 2025

*Keywords*:
Cancer
Biopsy
Diagnosis
Artificial Intelligence
Melanoma
Research precision

ABSTRACT

Millions of individuals throughout the world are afflicted by the devastating and difficult disease of cancer. Effective cancer therapy and better patient outcomes depend on early detection. To detect cancer, numerous methods have recently been created and put to use. Each method has advantages, disadvantages, and possible uses. Traditionally the detection was done through visual analysis resulting in delayed detection. In this article an automated model based on model development using deep learning for skin cancer detection is proposed. Recent developments in machine learning and computer vision techniques have demonstrated encouraging results in automating the identification of skin cancer using dermoscopy images, supporting dermatologists in their diagnostic procedure. The testing of VGG-19 models for different learning results in selection of highly efficient model for skin cancer detection. The proposed technique successfully distinguished between malignant and benign skin lesions with prominent performance in terms of accuracy, highlighting its potential as an accurate diagnostic tool for research precision.

## 1. INTRODUCTION

Cancer is a genetically based disease that is characterized by unchecked cell proliferation and dissemination. It is a diverse illness condition that is responsible for the second prominent reason of mortality. Because it affects so many cellular physiological systems, the sickness is extremely difficult to comprehend.

The use of nanotechnology in cancer biology has given researchers hope for the future of developing cutting-edge cancer therapy approaches. According to [1, 2] numerous nano constructions have been created from natural sources using physical or chemical techniques, revolutionizing the delivery of cancer-fighting medications with regard to medicinal applications. Numerous natural substances have been studied for their potential as anti-cancer agents, including polyphenols, polypeptides, metallic complexes, and polysaccharides. Among them, polysaccharides are a very adaptable group of biopolymers with exceptional structural qualities and exceptional biological functions.

*Challenges in Detecting Cancer:*

There are several challenges in detecting cancer, which include:

*Early detection*: One of the biggest challenges in detecting cancer is to identify it at an early stage. Many cancers are asymptomatic in their early stages and may only become symptomatic once they have advanced, making early detection more difficult.

*Reliable diagnostic tools*: Another challenge is to develop reliable diagnostic tools that are both accurate and affordable. Currently, biopsy and medical imaging are the main methods used to diagnose cancer, but these methods have limitations, such as being invasive or having low sensitivity.

*Overdiagnosis and overtreatment*: There is a risk of overdiagnosis and overtreatment of cancer, where individuals are diagnosed with cancer when they may not actually have it, or where treatments are given when they may not be necessary. This can lead to physical, emotional, and financial harm to patients.

*Personalized treatment*: The complexity and diversity of cancer makes it difficult to develop personalized treatments that are effective for all patients. There is a need for improved diagnostic tools and algorithms that can help to tailor treatments to individual patients.

[1]*Department of CSE, Chandigarh University, Gharuan, Punjab, India.*
[2]*Department of ECE, Chandigarh University, Gharuan, Punjab, India.*
[3]*Marwadi University Research Centre, Department of Engineering, Marwadi University, Rajkot, Gujarat, India*
[4]*Chitkara University Institute of Engineering and Technology, Chitkara University, Punjab, India.*
[5]*College of Dentistry, National University of Science and Technology, Dhi Qar, Iraq.*
[6]*Medical Technical College, Al-Farahidi University, Iraq.*
**Corresponding Author:* Vinay Kukreja; Phone: +919803825400; Email: onlyvinaykukreja@gmail.com.

*Lack of large and diverse datasets*: Another challenge is the lack of large, diverse, and annotated datasets for cancer detection and diagnosis. This limits the ability of machine learning algorithms to accurately detect and diagnose cancer, and results in lower accuracy rates.

*Bias in AI algorithms*: Bias can occur in AI algorithms that are used for cancer detection and diagnosis, leading to unequal and unjust results for certain populations. It is important to ensure that AI algorithms are developed and validated in a way that minimizes bias.

*Categories of Cancer Diseases:*

There are several types of cancer, each affecting different parts of the body. Some of the most common types of cancer include:

a. *Carcinoma*: Majorly it affects the skin and underlying tissues that line the internal organs. Examples include breast, lung, and prostate cancer.
b. *Sarcoma*: Affects the bones, cartilage, and tissues that connect and support the body. Examples include osteosarcoma and chondrosarcoma.
c. *Leukemia*: Affects the blood cells and bone marrow.
d. *Lymphoma*: Affects majorly the lymphatic system.
e. *Central Nervous System (CNS) Tumors*: This type of cancer affects the brain and spinal cord. Examples include gliomas and meningiomas.
f. *Melanoma*: Affects the skin cells that produce pigment.
g. *Gastrointestinal Cancers*: Affects the digestive system, including the stomach, intestines, liver, and pancreas. Examples include colorectal, pancreatic, and gastric cancer.

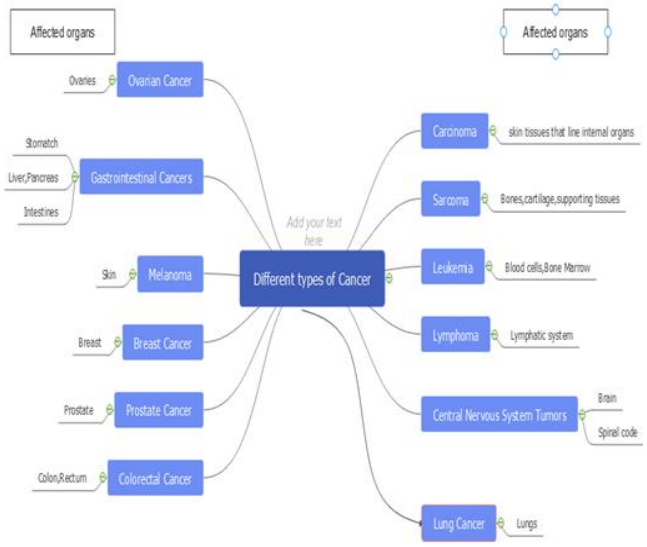


**Fig. 1. Commonly Affected Organs by Various Types of Cancer.**

In Figure 1 we have explained different types of cancers that affect different body organs of humans and further we will discuss how we have to rectify these types of diseases.

*Facts regarding Cancer disease:*

The National Cancer Institute (NCI) is a government organization that manages and funds cancer research as well as the American National Cancer Programmed. The latest NCI statistics show that since 2013, the incidence of cancer has been largely steady in the United States, with about 1.8 million new cases and more than 600,000 cancer-related deaths expected in 2020. With an anticipated 135,720 deaths from cancer in 2020, lung and bronchus cancer will be the main cause of death from cancer in both men and women. The mortality rates for lung cancer have, however, been declining for the past 20 years as a result of a decline in smoking rates and advancements in therapy.

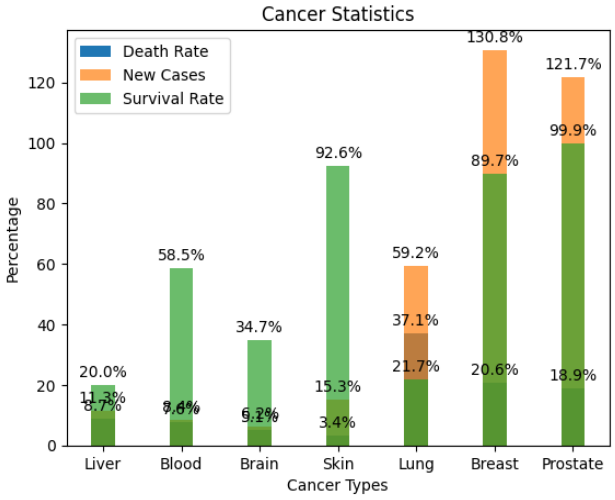


**Fig. 2. Cancer Types Based on National Cancer Institute Data.**

With an anticipated 280,000 new cases in 2020, breast cancer will be the most prevalent illness in women. However, the statistics regarding number of deaths due to breast cancer have also been dropping due to earlier detection through screening and improved treatments. With over 190,000 new cases in 2020, prostate cancer is the most prevalent cancer in men. The death rate from prostate cancer has been declining as a result of early discovery through screening and advancements in therapy, despite the fact that the incidence rate has been steady. With a projected 42,000 new instances of liver cancer in 2020, the disease has been on the rise. The high prevalence of hepatitis C and B virus infections, which are significant risk factors for liver cancer, is largely to blame for this rise in incidence.

With an expected 5 million new cases in 2020, the major type of cancer prevailing in US is skin cancer. Non-melanoma skin cancers, which make up the majority of skin cancers, are extremely curable if found and treated quickly. With an estimated 24,530 new occurrences in 2020, malignancies of the nervous system, including those of the brain, are rather uncommon. However, they have a generally

low survival rate, are frequently aggressive, and are challenging to treat. The statistics for different types of cancers are demonstrated through Figure 2.

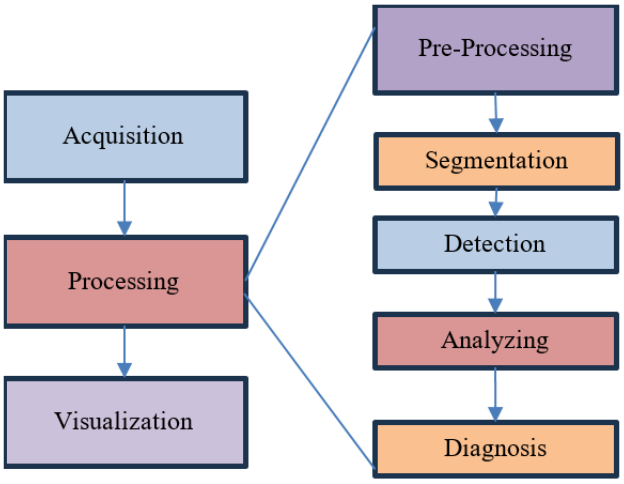


**Fig. 3. CAD process for cancer detection.**

*Schematic process for computer aided diagnosis of Cancer*

A systematic approach using computational algorithms and techniques to assist in the identification and diagnosis of cancer is part of the computer-aided diagnosis (CAD) process schematic. The procedure can be broken down into many crucial parts.

The data collection, pre-processing, image segmentation, feature extraction, classification, validation, and integration into clinical practice are all included in the schematic process for CAD of cancer. It blends cutting-edge computational methods with medical knowledge to support precise and effective cancer detection.

*Skin cancer detection:*

Detecting the existence of malignant cells or lesions on the skin is referred to as the skin cancer detection method. Skin cancer is one of the most common types of cancer, and it can develop due to a range of factors, including exposure to ultraviolet (UV) radiation from the sun or tanning beds, genetic mutations, and environmental toxins. The most common types of skin cancer are basal cell carcinoma [4], squamous cell carcinoma, and melanoma [5]. Early detection of skin cancer is critical for improving patient outcomes and survival rates. Diagnosis of skin cancer typically involves a combination of visual examination of the skin, dermoscopy and biopsy.

Structure of skin layers: The skin is made up of three main layers, each of which has a distinct structure and purpose.

The epidermis, or top layer, is what helps to create skin cells. It serves as a barrier and guards against pathogens entering your body. The middle layer of skin, or dermis, is the second layer and is composed of elastin, which gives skin its flexibility, and collagen, which gives skin cells strength. The hypodermis, which makes up the bottom layer of skin, controls body temperature and safeguards bones and muscles from harm. Structure of skin is shown below in Figure 4.

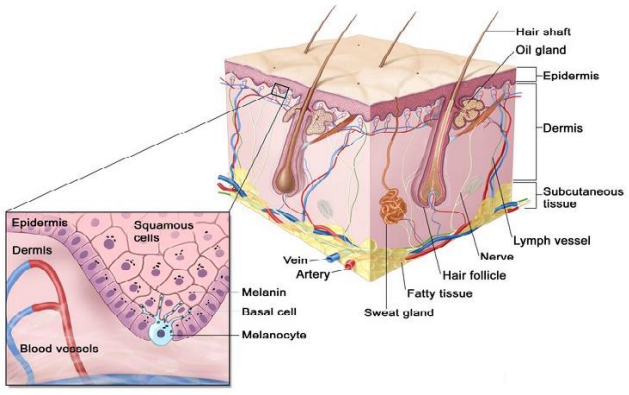


**Fig. 4. Classification of Skin layers in human body [6]**

Cells in our body grow and divide for the whole life. But if these normal cells are infected, they have uncontrolled and undesirable division. These cancer cells grow in whole body for whole life. Cancer takes birth with these infected cells. After sometime this production is out of control and then it can invade in to the other parts of body through blood stream of lymph nodes.

*Stages of Skin cancer:*

Cancer has basically four stages.

*Stage A*: there is no cancer. There are only abnormalities in cells which can take birth to the cancer. This is known as carcinoma in situ.

*Stage B*: cancer is very weak and it resides in only one area. It is also called early stage.

*Stage C*: cancer is large now and has infected the tissues.

*Stage D*: cancer has infected the lymph nodes and blood stream

*Stage E*: cancer has entered in to the other parts of the body. This is known as metastasis or advanced cancer. Cancer stages are shown in Figure 5.

This paper proposed an upgraded VGG19 model by adding 2 extra layers and 128 filters to identify and classify the skin lesions as malignant or benign accurately. Data has been collected from various sources and it has been tested through a rigorous process by dividing the data into 80:20 ratios for testing and training purposes. This study contributes to the advancement of automated diagnostic tools in dermatology, which could improve patient outcomes through timely intervention. After comparative analysis of results with the existing methods it has been concluded that VGG19 is better than CNN and other models.

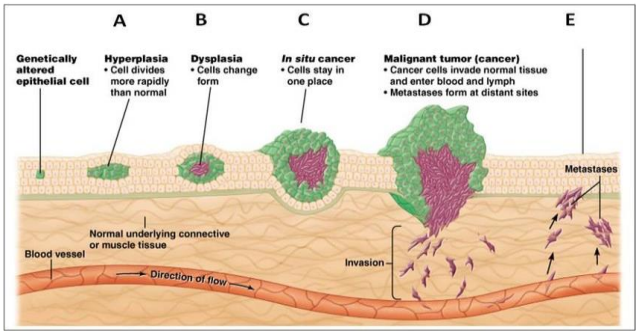


**Fig. 5. Phases of cancer [7].**

## 2. LITERATURE REVIEW

A variety of deep learning approaches have been proposed to improve the classification and diagnosis of skin lesions. One such method is the CNN-based gradient boosting technique designed with a focus on dermatology and artificial intelligence [8]. This model utilized 37 binary classifications to differentiate between biopsy-verified benign and malignant tumors using dermoscopy images derived from clinical and histological sources. Similarly, a hierarchical stacking ensemble using meta-learning and generative adversarial networks was developed to analyze PH2 and Gangster-based datasets with five-fold cross-validation [9]. An IoT-compatible model integrating deep learning was also introduced to provide reliable, objective diagnoses for skin cancer classification [10]. Furthermore, a real-time neural network framework employing ResNet was described for enhanced classification accuracy [11], while an ensemble-based, multi-scale CNN model was employed to augment images and improve categorization across lesion types [12]. These methods were complemented by multi-modal imaging approaches for improved discrimination between benign and malignant tumors [13].

In terms of clinical observation, early detection remains crucial. The presence of irregular or evolving moles-often appearing on the arms, legs, or face-can be a strong indicator of melanoma, a form of skin cancer once considered incurable [14]. Advances in melanoma diagnosis have led to greater awareness among healthcare professionals, especially concerning symptoms such as painful or scaly patches. While certain demographic groups, such as Blacks and Hispanics, may have higher incidence rates, melanoma affects a broad population spectrum. Supporting these efforts, dermoscopic images have become an important diagnostic aid [15], and publicly available datasets like MEDNODE and ISIC are commonly used for CAD model training and validation [16, 17].

Several studies have leveraged these datasets to build robust skin lesion classifiers. For example, the MED-NODE system, utilizing non-dermoscopic images, was found to outperform other automated approaches [18]. Investigations into image quality metrics such as MSE, PSNR, and SSIM showed that preprocessing methods-like anisotropic diffusion and sigmoid filtering-could enhance lesion visibility [19]. Thresholding techniques applied to high-resolution dermoscopic datasets also contributed to lesion border detection and malignancy identification [20]. However, certain noise reduction strategies like Dmey filtering showed limitations under low-light conditions [21].

Image enhancement and segmentation remain vital components of diagnostic models. Techniques such as multi-scale retinex and contrast restoration have improved lesion visualization and classification accuracy [22]. CNN-based image enhancement and dimensional transformations also contributed to performance gains on datasets with over 500 dermoscopic images [23]. Further, interpolation and pixel-class accumulation were applied to reconstruct lesion images, enabling better morphological analysis [24–26]. These restoration strategies required balancing between image fidelity and model flexibility.

More advanced architectures have also been explored. Recurrent Neural Networks (RNN) and Deep Autoencoders were utilized to model sequential patterns and reduce functional dimensions in lesion images [29]. Sparse and de-noising variants of autoencoders added further adaptability despite lacking pre-training protocols [30]. However, CNN-based architectures like ResNet, VGG, and AlexNet-though powerful-are often computationally intensive and require complex model design [31–33]. Finally, skin type classification using the Fitzpatrick scale was incorporated into large-scale image datasets to support model generalization across diverse populations [34].

## 3. MATERIALS AND METHODS

### *3.1. Dataset for skin cancer detection*

Images are gathered from many websites. There are two distinct image categories in the Dermquest dataset: nevus and melanoma. The 100 nevi and 70 melanoma image sets in the med-node dataset.

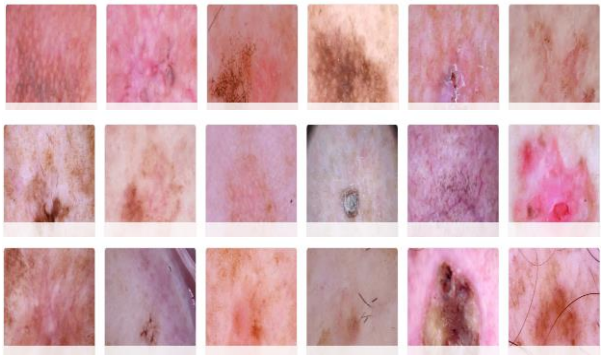

**Fig. 6. Data Set of nevus and melanoma images.**

For the current analysis, images classified as benign (19373 images) and malignant (2285 images) were acquired from the International Skin Imaging Collaboration (ISIC) collection. Another dataset is the dermis dataset. There are

40 melanoma photos and 160 nevi images in the Ph2 dataset. For the current investigation, a total of 13,000 images-10,000 benign and 3,000 malignant-were used. Sample images are shown in figure 6.

### *3.2. Proposed model*

The VGG-19 model is a highly efficient and pre-trained architecture for performing classification tasks on image dataset [35], and its performance is slightly better than that of other models like ResNet and Alexnet [36]. Figure 7 shows the VGG-19 model's architecture, which consists of 16 convolutional layers, 5 pooling layers, and 3 dense layers. The volume size is 224*224*64 and is produced by 64 filters with a stride of "1" and two preamble layers that are referred to as convolutional layers.

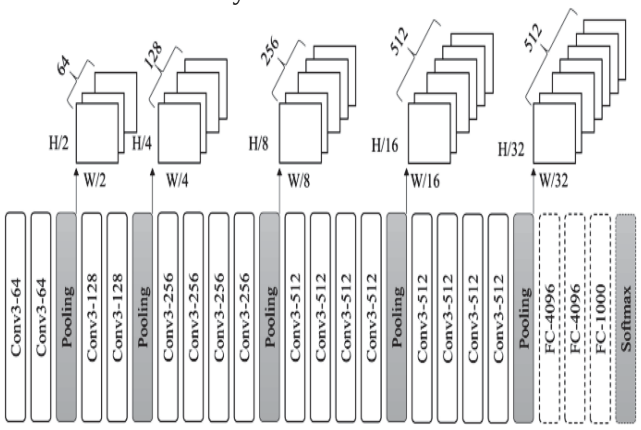


**Fig. 7. VGG-19 Layers.**

To minimize the height and breadth volume to 112*112*64, the pooling layer is then involved with a 2*2 size of max-pool with a stride of "2". This new volume result is further convolved using 2 more layers and 128 filters, yielding a dimension result of 112*112*128. Next, the dimension is decreased to 56*56*256 using the pooling layer's concern. Additionally, 2 more convolutional layers are added, the filter size is increased to 512, and the dimension is decreased to 28*28*512 via down sampling. The result of the soft max is 1000 in classes (1*1*1000) and the volume of the last pooling layer is 7*7*512. It is firmed into a fully linked layer with a channel size of 4096. The training modes for the output layer (VGG-19 model) are (i) image enhancement, (ii) training and assessment, (iii) running the model, and (iv) compilation.

The labels are encoded over the melanoma photos for the target model. Train, test, and validation datasets are created from the datasets. The dataset size for training, testing, and validation is 30000. The random state in this case is set to 30. In this example, the basic model (VGG- 19 in this case) has a dropout of 0.2 and a SoftMax activation function. Additionally, for improved classification accuracy, two dense layers of sizes 256 and 128 employ cross-entropy loss and batch sizes of 100. To evaluate the model's performance, the base parameter settings from the reference paper are used. We employ various learning rates in the VGG model for multiclass melanoma classification, notwithstanding the reference's use of 0.0001. For a learning rate of 0.0001, this model's accuracy is 98.61. In this case, there are 100 epochs and 300 iterations. The model reaches convergence at the 12th epoch. Therefore, for the purposes of our inquiry, the number of epochs is lowered to 30, and the model's performance is examined. Because there are so many training, testing, and validation datasets, we introduced momentum of 0.9 to help the model converge more quickly. Table provides a performance analysis of the VGG-19 model for melanoma classification.

**Table 1: Probability of disease**

| Input | Have the disease | Does not have the disease |
|---|---|---|
| Have the cancer (c) | True positive- -$n_{c\to c}$ | False Positive - $n_{c\to nc}$ |
| Does not have the cancer (nc) | False negative - $n_{nc\to c}$ | True Negative - $n_{nc\to nc}$ |

**Table 2: Equations of performance parameters**

| Performance Metric | Evaluation Function |
|---|---|
| Accuracy | $\boldsymbol{ACC} = \frac{\boldsymbol{n_{c\to c} + n_{nc\to nc}}}{\boldsymbol{n_{c\to c} + n_{nc\to nc} + n_{nc\to c} + n_{c\to nc}}}$ |
| True positive rate/ Recall/ Sensitivity (TPR) | $\boldsymbol{TPR} = \frac{\boldsymbol{n_{c\to c}}}{\boldsymbol{n_{c\to c} + n_{nc\to nc}}}$ |
| False positive rate (FPR) | $\boldsymbol{FPR} = \frac{\boldsymbol{n_{c\to nc}}}{\boldsymbol{n_{c\to nc} + n_{nc\to nc}}}$ |
| Positive prediction value / Precision (PPV) | $\boldsymbol{PPV} = \frac{\boldsymbol{n_{c\to c}}}{\boldsymbol{n_{nc\to nc} + n_{c\to c}}}$ |
| False Negative rate (FNR) | $\boldsymbol{FNR = 1 - TPR}$ |
| F1 score | $\mathbf{f1} = \frac{\boldsymbol{2 * TPR * PPV}}{\boldsymbol{TPR + PPV}}$ |

## 4. RESULTS AND DISCUSSION

For performance evaluation the parameters listed in table 1 are evaluated for the proposed model. The mathematical expressions used to calculate parameters are derived from the confusion matrix. The binary prediction test needs to meet the performance criteria of sensitivity and specificity. It can be seen that the sensitivity (SN) was calculated as the proportion of anomalous images that were correctly identified to the sum of all the input image data. The specificity (SP) represents the ratio of correctly diagnosed normal images to the ratio of all available normal test images

of input image data, i.e., it can identify the healthy people who do not have the disease.

It indicated the probability of sick people who are correctly predicted with disease. referred to as a negative rate.

**Table 3: Performance analysis of VGG-19 model**

| Model | Learning rate | Precision | Recall | Accuracy | F1 score | MCC | Jaccard Index |
|---|---|---|---|---|---|---|---|
| TL using VGG-19 | 0.1 | 56.78 | 56.23 | 55.89 | 56.50 | 55.41 | 55.12 |
| | 0.01 | 65.12 | 63.87 | 63.44 | 64.49 | 63.54 | 63.01 |
| | 0.001 | 73.24 | 72.16 | 69.89 | 72.70 | 68.99 | 68.86 |
| | 0.0001 | 97.23 | 98.89 | 98.61 | 98.05 | 98.99 | 98.93 |
| | 0.00001 | 89.65 | 89.32 | 88.64 | 89.48 | 88.54 | 88.41 |
| | 0.000001 | 42.13 | 41.87 | 41.32 | 42.00 | 41.12 | 41.01 |

The accuracy (ACC) ratio, which is measured for each case, is the difference between the normal and abnormal categorization images. The classification of the image as normal or abnormal was examined. The classifier was taught to distinguish between normal and abnormal predictions. The two categories linked to the classification process are abnormal and normal. When the output of a neural network was compared to datasets of normal and abnormal images, the outcome predictions were calculated for a set of samples.

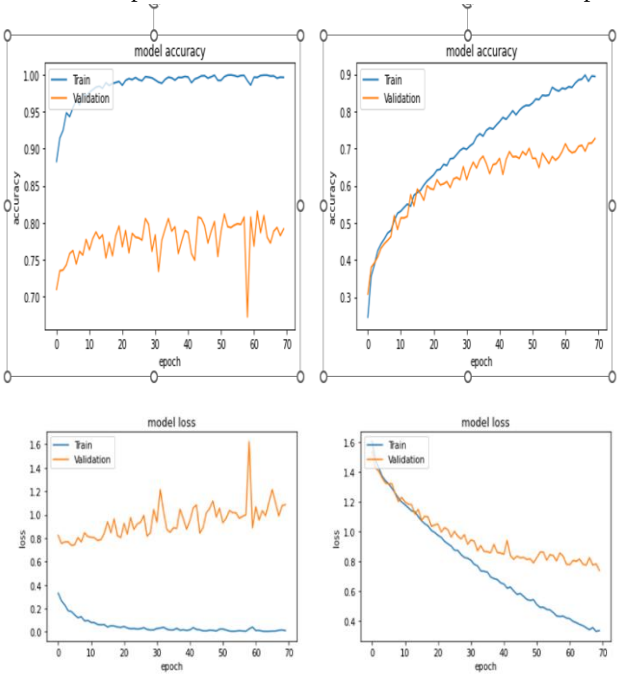


**Fig. 8. Training and Testing Accuracy graph and Figure 9: Training and Testing Loss graph.**

To evaluate network performance, the trained model is tested with unknown set of images thereby performing well in terms of accuracy. The accuracy throughout training and testing was 0.985 and 0.975, respectively. While the losses during testing and training were, respectively, 0.099 and 0.119. The variation of accuracy and loss for training and validation over time, from the first training period to the final is shown in Figures 8 and 9.

## 5. CONCLUSIONS

The classification of the cancer types Skin cancer, was discussed, presented, and evaluated in this research. TL and CNN built on the VGG19 platform have shown to be effective tools for highly accurate skin cancer diagnosis. The interpretability of the VGG-19 model also provides information on the characteristics that affect its judgements. The overall accuracy during training and testing using VGG_19 model was 0.985 and 0.975, respectively. The losses during testing and training were 0.119 and 0.099, respectively. Accuracy and loss for training and validation vary over time. Our findings show that the VGG19 model was highly accurate, sensitive, and specific in differentiating between different types of skin lesions. This shows that it could be a beneficial tool for early identification and diagnosis of skin cancer, allowing medical professionals to make more informed decisions about patient care. However, despite its promising performance, there are certain restrictions to consider. One such limitation is the necessity for a large dataset with various samples to assure the model's robustness and generalization. Furthermore, future research might focus on refining the model architecture and fine-tuning hyper-parameters to increase performance even further. As a result of the system's increased credibility and confidence-boosting effects, it is more widely adopted and integrated into standard therapeutic procedures. To improve the training accuracy even more, additional pre-processing measures might be implemented, such as hair removal

## REFERENCES

[1] Liu, Y.; Gao, X.; Zhou, J.; Zheng, X.; Zou, R.; Xu, X.; Yu, X.; Li, J. 2019. Hepatocellular carcinoma: Diagnostic performance of multidetector CT and MR imaging-a systematic review and meta-analysis. *Radiology* 292(4): 79–94. doi: 10.1148/radiol.2019182387.

[2] Li, B.; Liu, X.; Li, C.; Mao, X.; Cai, J.; Li, W.; Yang, G.; Liu, J.; Ding, J.; Bai, C. 2020. Combination of radiomics and machine learning for diagnosis of hepatocellular carcinoma. *Aging (Albany NY)* 12(23): 24067–24084. doi: 10.18632/aging.202458.

[3] National Cancer Institute. Types of skin cancer. Accessed on 12 January 2023 from https://www.cancer.gov/types/skin

[4] Ansari, U.B.; Sarode, T. 2017. Skin cancer detection using image processing. *International Research Journal of Engineering and Technology* 4: 2875–2881.

[5] Hoshyar, A.N.; Al-Jumaily, A.; Hoshyar, A.N. 2014. The beneficial techniques in the preprocessing step of skin cancer detection system comparing. *Procedia Computer Science* 42: 25–31.

[6] National Cancer Institute. The Cancer Genome Atlas.

Accessed on 12 January 2023 from https://www.cancer.gov/tcga

[7] Munir, K.; Elahi, H.; Ayub, A.; Frezza, F.; Rizzi, A. 2019. Cancer diagnosis using deep learning: A bibliographic review. *Cancers* 11(9): 1235. https://doi.org/10.3390/cancers11091235

[8] Hekler, A.; Utikal, J.S.; Enk, A.H.; Hauschild, A.; Weichenthal, M.; Maron, R.C.; Berking, C.; Haferkamp, S.; Klode, J.; Schadendorf, D.; Schilling, B. 2019. Superior skin cancer classification by the combination of human and artificial intelligence. *European Journal of Cancer* 120: 114–121.

[9] Ghalejoogh, G.S.; Kordy, H.M.; Ebrahimi, F. 2020. A hierarchical structure based on stacking approach for skin lesion classification. *Expert Systems with Applications* 145: 113127.

[10] Rodrigues, D.D.; Ivo, R.F.; Satapathy, S.C.; Wang, S.; Hemanth, J.; Reboucas Filho, P.P. 2020. A new approach for classification skin lesion based on transfer learning, deep learning, and IoT system. *Pattern Recognition Letters* 136: 8–15.

[11] Harangi, B.; Baran, A.; Hajdu, A. 2020. Assisted deep learning framework for multi-class skin lesion classification considering a binary classification support. *Biomedical Signal Processing and Control* 62: 102041.

[12] Mahbod, A.; Schaefer, G.; Wang, C.; Dorffner, G.; Ecker, R.; Ellinger, I. 2020. Transfer learning using a multi-scale and multi-network ensemble for skin lesion classification. *Computer Methods and Programs in Biomedicine* 193: 105475.

[13] Amin, J.; Sharif, A.; Gul, N.; Anjum, M.A.; Nisar, M.W.; Azam, F.; Bukhari, S.A. 2020. Integrated design of deep features fusion for localization and classification of skin cancer. *Pattern Recognition Letters* 131: 63–70.

[14] Thau-Zuchman, O.; Ingram, R.; Harvey, G.G.; Cooke, T.; Palmas, F.; Pallier, P.N.; Brook, J.; Priestley, J.V.; Dalli, J.; Tremoleda, J.L.; et al. 2020. A single injection of docosahexaenoic acid induces a pro-resolving lipid mediator profile in the injured tissue. *Journal of Neurotrauma* 37: 66–79.

[15] Haider, S.T. et al. 2021. Illustration and identification of skin lesions in dermoscopic dataset using pattern recognition techniques. In: Tavana, M.; Nedjah, N.; Alhajj, R. (Eds.) *Emerging Trends in Intelligent and Interactive Systems and Applications*. IISA 2020. *Advances in Intelligent Systems and Computing* 1304. Cham: Springer. https://doi.org/10.1007/978-3-030-63784-2_118.

[16] Mukherjee, S.; Adhikari, A.; Roy, M. 2020. Malignant melanoma detection using multilayer perceptron with PCA components from MED-NODE dataset. *International Journal of Medical Engineering and Informatics* 12: 151-168.

[17] Mahbod, A.; Schaefer, G.; Wang, C.; Dorffner, G.; Ecker, R.; Ellinger, I. 2020. Transfer learning using a multi-scale and multi-network ensemble for skin lesion classification. *Computer Methods and Programs in Biomedicine* 193: 105475.

[18] Varkentin, A.; Mazurenka, M.; Blumenröther, E.; Behrendt, L.; Emmert, S.; Morgner, U.; Meinhardt-Wollweber, M.; Rahlves, M.; Roth, B. 2018. Trimodal system for in vivo skin cancer screening. *Journal of Biophotonics* 11: e201700288.

[19] Sau, K.; Maiti, A.; Ghosh, A. 2018. Preprocessing of skin cancer using anisotropic diffusion and sigmoid function. In: *Advanced Computational and Communication Paradigms*. Springer: 51–61.

[20] Sankaran, S.; Sethumadhavan, G. 2018. Entropy-based colour splitting in dermoscopy images. *Proc. Int. Conf. on Inventive Research in Computing Applications (ICIRCA)*. Coimbatore, India, pp. 771–774. doi: 10.1109/ICIRCA.2018.8597177.

[21] Arora, G.; Dubey, A.K.; Jaffery, Z.A. 2019. Design of Dmey Wavelet Gaussian Filter (DWGF) for de-noising of skin lesion images. In: *Smart Innovations in Communication and Computational Sciences*. Springer: 475–484.

[22] Pandey, P.; Saurabh, P.; Verma, B.; Tiwari, B. 2019. A multi-scale retinex with color restoration technique for skin cancer detection. In: *Soft Computing for Problem Solving*. Springer: 465–473.

[23] Aima, A.; Sharma, A.K. 2019. Predictive approach for melanoma skin cancer detection using CNN. *Proc. Int. Conf. on Sustainable Computing in Science, Technology and Management (SUSCOM)*, Jaipur, India, February 26–28. SSRN: https://ssrn.com/abstract=3352407.

[24] Harangi, B. 2018. Skin lesion classification with ensembles of deep convolutional neural networks. *Journal of Biomedical Informatics* 86: 25–32.

[25] Dorj, U.-O.; Lee, K.-K.; Choi, J.-Y.; Lee, M. 2018. Skin cancer classification using deep convolutional neural network. *Multimedia Tools and Applications* 77: 9909–9924.

[26] Ghalejoogh, G.S.; Kordy, H.M.; Ebrahimi, F. 2020. A hierarchical structure based on stacking approach for skin lesion classification. *Expert Systems with Applications* 145: 113127.

[27] Öztürk, Ş.; Özkaya, U. 2020. Skin lesion segmentation with improved convolutional neural network. *Journal of Digital Imaging* 33: 958–970.

[28] Aishwarya, U.; Daniel, I.J.A.C.K.S.O.N.; Raghul, R. 2020. Convolutional neural network-based skin lesion classification and identification. *Proc. Int. Conf. on Inventive Computation Technologies (ICICT)*.

[29] Divya, D.; Ganeshbabu, T.R. 2020. Fitness adaptive deer hunting-based region growing and recurrent neural network for melanoma skin cancer detection. *International Journal of Imaging Systems and Technology* 30: 731–752.

[30] Sabbaghi, S.; Aldeen, M.; Garnavi, R. 2016. A deep bag-of-features model for the classification of melanomas in dermoscopy images. *Proc. IEEE Engineering in Medicine and Biology Society (EMBC)*.

[31] Hosny, K.M.; Kassem, M.A.; Foaud, M.M. 2019. Classification of skin lesions using transfer learning and augmentation with AlexNet. *PLoS One* 14: e0217293.

[32] Amin, J.; Sharif, A.; Gul, N.; Anjum, M.A.; Nisar, M.W.; Azam, F.; Bukhari, S.A.C. 2020. Integrated design of deep features fusion for localization and classification of skin cancer. *Pattern Recognition Letters* 131: 63–70.

[33] Demir, A.; Yilmaz, F.; Kose, O. 2019. Early detection of skin cancer using deep learning architectures: ResNet-101 and Inception-V3. *Proc. Medical Technologies Congress (TIPTEKNO)*, Izmir, Turkey, pp. 1–4. doi: 10.1109/TIPTEKNO47231.2019.8972045.

[34] Holm-Schou, A.-S.S.; Philipsen, P.A.; Wulf, H.C. 2019. Skin cancer phototype: A new classification directly related to skin cancer. *Photodermatology, Photoimmunology & Photomedicine* 35: 116–123.

[35] Uoc, N.Q.; Duong, N.T.; Son, L.A.; Thanh, B.D.A. 2022. Novel automatic detecting system for cucumber disease based on the convolution neural network algorithm. *GMSARN International Journal* 16: 295–301.

[36] KS, A.K.; Sarita, K.; Kumar, S.; Saket, R.K.; Swami, A. 2022. Machine learning-based approach for prevention of COVID-19 using steam vaporizer. *GMSARN International Journal* 16: 399–404.